Cross-Sectional Imaging Findings of Atypical Liver Malignancies and Diagnostic Pitfalls

Emphasis on Computed Tomography, and Magnetic Resonance Imaging

Michael J. King, MD[a], Indira Laothamatas, MD[a], Arthi Reddy, MD[a], Rebecca Wax, MD[a], Sara Lewis, MD[a,b,*]

KEYWORDS

• Liver malignancy • Hepatocellular carcinoma • Metastases • Sarcoma • Computed tomography • Magnetic resonance imaging

KEY POINTS

- Atypical liver malignancies, which may be defined as either an atypical appearance of commonly encountered lesions or lesions that are encountered rarely, pose diagnostic challenges at cross-sectional imaging.
- Knowledge of key imaging findings and differential diagnostic considerations can aid in making an accurate diagnosis.

INTRODUCTION

Advances in cross-sectional imaging methods with computed tomography (CT) and magnetic resonance imaging (MRI) have improved the radiologist's ability to noninvasively characterize many liver malignancies with high accuracy. Recent developments include improvements in imaging technique, sequences, protocols, use of newer liver-specific contrast agents (ie, gadoxetic acid for MRI), as well as the incorporation of functional and/or quantitative methods (ie, diffusion-weighted MRI) into routine imaging protocols.

Malignant liver lesions include lesions that originate in the liver (primary) and lesions that are metastatic from other organs (secondary). Often, patients are either asymptomatic or have nonspecific symptoms, and thus present with advanced disease at the time of diagnosis. Apart from hepatocellular carcinoma (HCC), intrahepatic cholangiocarcinoma (ICC), and hepatic metastases, other types of malignant liver lesions are quite rare.[1] As such, despite improvements in imaging methods, atypical liver malignancies, which may be defined as either an atypical appearance of commonly encountered lesions or lesions that are encountered rarely, remain challenging to characterize on imaging. While primary liver malignancies such as HCC, and to a lesser extent ICC, have characteristic and well-described imaging appearances, atypical presentations exist, such as infiltrative, cystic, or intraductal HCC or

[a] Department of Diagnostic, Molecular and Interventional Radiology, Icahn School of Medicine at Mount Sinai, Box 1234. New York, NY 10029, USA; [b] BioMedical Engineering and Imaging Institute, Icahn School of Medicine Mount Sinai, 1470 Madison Avenue, New York, NY 10029, USA

* Corresponding author. One Gustave Levy Place, Department of Diagnostic, Molecular and Interventional Radiology, Icahn School of Medicine at Mount Sinai, Box 1234. New York, NY 10029.

E-mail address: sara.lewis@mountsinai.org

Radiol Clin N Am 60 (2022) 775–794

https://doi.org/10.1016/j.rcl.2022.05.003

mucinous ICC.[2] The increasingly recognized entity combined hepatocellular-intrahepatic cholangiocarcinoma (cHCC-ICC) is notoriously difficult to diagnose preoperatively or without histologic confirmation.[3] Clearly, accurate diagnosis is essential, as the management and prognosis of these lesions differ drastically. On the other hand, certain hepatic malignancies, such as primary neuroendocrine malignancy, mesenchymal sarcomas, and hematologic malignancy, occur so rarely and are highly variable in appearance, contributing to the challenge of making an accurate diagnosis. Furthermore, certain benign lesions and pseudotumors, such as inflammatory pseudotumor, vascular shunting, focal or confluent hepatic fibrosis, and focal fat deposition can mimic malignancy, especially in oncologic patients or patients at risk for HCC.[4]

Diagnostic radiologists are playing an increasingly important role in the interdisciplinary care of patients. Knowledge of the epidemiologic factors, certain cross-sectional imaging appearances, and key technical and imaging pitfalls can contribute significantly to accurate diagnosis and subsequent patient management. In this article, we review certain technical considerations and focus on atypical appearances of common primary and secondary malignant liver lesions, as well as uncommon malignant liver lesions, with emphasis on CT and MRI.

TECHNICAL PITFALLS

Imaging Technique Considerations

Careful attention to imaging protocol and acquisition technique is essential to enabling accurate liver lesion characterization. Dedicated imaging protocols have been developed and optimized for both CT and MRI, details of which are reported elsewhere.[5,6] Pre/postcontrast imaging is the cornerstone of focal liver lesion detection and characterization, and liver scanning protocols routinely include noncontrast, late arterial phase (AP), portal venous phase (PVP), and equilibrium (EP) or transitional phase (TP) or delayed phase (DP) using either extra-cellular contrast agents (CT and MRI) or liver-specific contrast agents (MRI; gadoxetic acid).

Late arterial phase is defined as hepatic artery enhancement as well as early enhancement of the portal vein, with no or minimal liver parenchymal enhancement, and is essential for the determination of arterial phase hyperenhancement (APHE) that is characteristic of certain hepatic malignancies.[5,7] Special attention to technique, timing, and image quality of late arterial phase MRI with gadoxetic acid is warranted, given the risk of transient severe motion (TSM) and that the small volume of agent administered may result in a shortened, less avid enhancement duration.[8,9] Finally, while CT scanning is less impacted by patient motion due to rapid acquisition time, voluntary and physiologic involuntary motion during longer-acquisition MRI can result in significant image degradation and artifacts—such as blurring and ghosting which cause image duplicates from misplaced signal—all of which may impede image interpretation.[10]

Image Interpretation Pearls

Uncommonly, HCC or hepatic metastases may contain hemorrhage (ie, RCC, neuroendocrine tumor, lung cancer, or choriocarcinoma) or melanin (ie, melanoma) resulting in T1 hyperintensity or hyperdensity on noncontrast MRI and CT, respectively.[4] Scrutiny of postcontrast subtraction MRI is then recommended to better define the lesion's enhancement characteristics. Registration between pre and postcontrast imaging is needed to avoid artifacts on subtraction imaging, which can be minimized by instructing patients on breath-holding technique. Unlike CT, breath-holding for MRI may be best performed on end-expiration to ensure a more consistent location of the diaphragm. For CT, careful manual region of interest (ROI) measurement or the use of dual-energy CT may be of value to determine enhancement within such lesions.[11]

The presence of moderate to severe steatosis or iron deposition in the background liver can potentially confound the characterization of focal liver lesions as the signal intensity of a lesion is evaluated and compared relative to the background parenchyma. It has also been reported that hepatic steatosis may potentially either mask or mimic liver metastases on CT in oncology patients.[12] Scrutiny of fat sensitive sequences, such as T1 in and opposed phase imaging or dedicated fat and iron quantification sequences on MRI, is recommended to recognize the presence of steatosis or iron deposition to ensure accurate characterization of liver lesions (**Fig.1**).[4]

PRIMARY LIVER CANCER

Hepatocyte Origin

Atypical hepatocellular carcinoma

According to international guidelines published by the American Association for the Study of Liver Diseases (AASLD), European Association for the Study of Liver (EASL) and Liver Reporting and Data System (LI-RADS), a liver lesion in the setting of cirrhosis with APHE followed by washout in the PVP or DP on CT or MRI is diagnostic for HCC without the need for pathologic confirmation.[13]

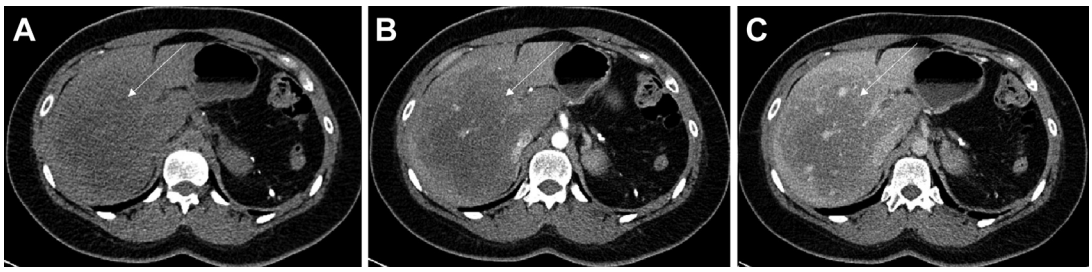

Fig. 1. 36-year-old woman with elevated liver function tests and mass-like hepatic steatosis. Axial noncontrast CT (*A*) demonstrates an ill-defined, mass-like region of decreased attenuation in the right hepatic lobe (*arrow*). The region of decreased attenuation in the right lobe measured 12 HU, compared with 57 HU in the left hepatic lobe. Postcontrast arterial phase (*B*) and portal venous phase (*C*) axial CTs demonstrate an ill-defined region of decreased attenuation in the right hepatic lobe without discrete mass (*arrows*), and otherwise normal background liver. Normal hepatic vessels are seen coursing through the hypoattenuating region without the evidence of mass effect.

However, these imaging criteria have reduced sensitivity (as low as 30%) for HCCs with atypical enhancement.[13] Atypical enhancement patterns are often seen in small and well-differentiated HCCs, and includes iso/hypovascular HCC (ie, without APHE), hypervascular HCC without PVP washout, and HCC that is hyperintense on the hepatobiliary phase (HBP) for MRI performed with liver-specific contrast agents (**Figs. 2** and **3**).[13] Isovascular or hypovascular lesions can be the first sign of early HCC, with a reported prevalence of 14% to 19.5%.[14] Choi and colleagues reported that 96.6% of hypovascular HCCs were also hypointense on the HBP, which, therefore, may be a hallmark of iso/hypovascular HCC.[15] Some HCCs are hypervascular on the AP without washout on the PVP, and there are conflicting studies on whether T2 hyperintensity can be seen as an indicator of HCC in these lesions.[13] Hypointensity on the HBP is a helpful finding but does not differentiate HCC from other lesions such as hepatic hemangiomas which also lack functioning hepatocytes.[16] Approximately 10% of HCCs are hyperintense on the HBP phase, while demonstrating the typical vascular enhancement profile on the dynamic phases of postcontrast imaging[13] However, 3% of HCCs that are hyperintense on the HBP phase may lack PVP or DP washout.[17] This can make it very difficult to distinguish atypical HCC from large regenerative nodules and other benign lesions, although scrutiny of the ancillary findings of T2 hyperintensity or restricted diffusion on diffusion weighted imaging (DWI) may be helpful for diagnosis.

Infiltrative hepatocellular carcinoma

Infiltrative HCC accounts for 7% to 20% of HCC cases and is almost always associated with cirrhosis.[18] The ill-defined appearance poses diagnostic challenges and can also mimic other liver diseases such as hepatic fat deposition, hepatic microabscesses, ICC, and diffuse metastatic disease.[18] Infiltrative HCC usually involves multiple hepatic segments, an entire hepatic lobe, or both lobes. Portal vein thrombosis is a very common finding with a frequency ranging from 68% to 100% and may often be the primary imaging feature.[18] On contrast-enhanced imaging, infiltrative HCC often has a permeative appearance, minimal and inconsistent arterial enhancement, and heterogeneous washout on the PVP. On MRI, the tumor is often heterogeneously T2 hyperintense, homogenously or heterogeneously T1 hypointense, and hyperintense on DWI compared with surrounding liver parenchyma (**Fig. 4**).[18]

Intraductal hepatocellular carcinoma

HCC will occasionally invade the bile ducts and cause bile duct tumor thrombus (BDTT) with a reported incidence of 0.53% to 12.9%.[19] The initial presentation may be obstructive jaundice and can mimic cholangiocarcinoma. Cholangiocarcinoma has a different surgical management from HCC with BDTT, and therefore, preoperative distinction is important, although is very challenging in the absence of liver parenchymal involvement. A retrospective study by Zhou and colleagues of pathologically proven HCC with hilar bile duct tumor thrombus (HBDTT) found that liver parenchymal involvement with an associated intraductal lesion, absence of hilar bile duct wall thickening, and washout in PVP were all found to have high sensitivity and high specificity for HCC with HBDTT.[19] Other imaging features with high specificity for HCC with HBDTT are vascular tumor emboli and splenomegaly. Clinical history of viral hepatitis and elevations of serum alpha-fetoprotein (AFP) level may also aid in the diagnosis.[19]

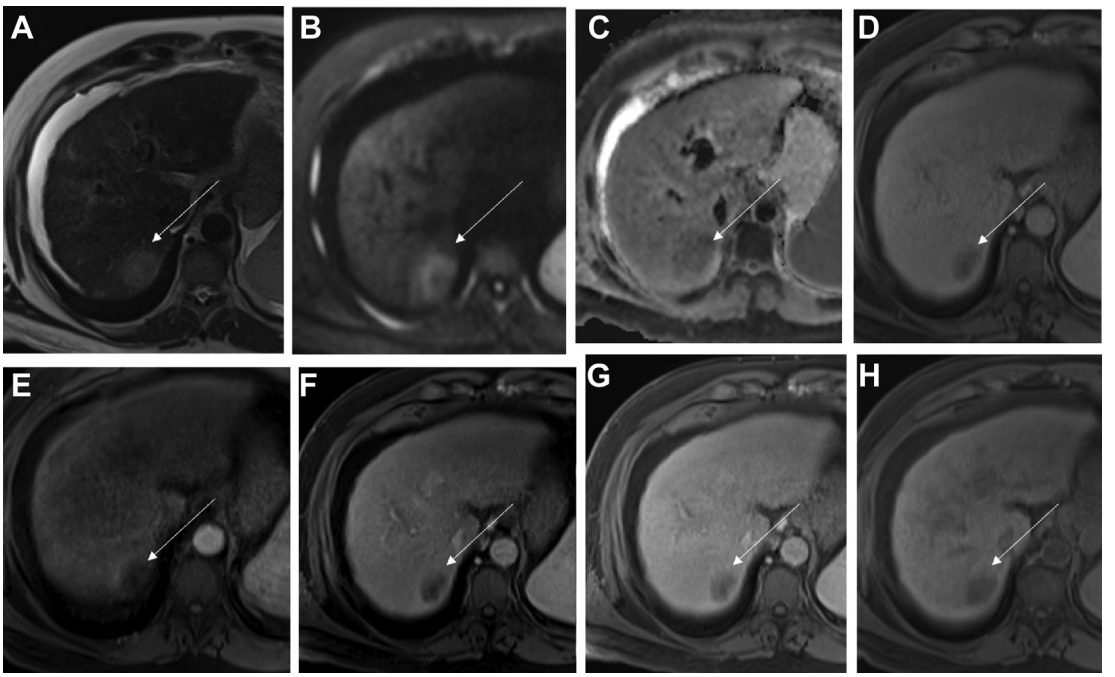

Fig. 2. 58-year-old man with nonalcoholic steatohepatitis undergoing HCC screening presenting with an atypical (hypovascular) HCC. Axial SS FSE T2WI (*A*) demonstrates a mildly T2 hyperintense, well-defined, ovoid mass in subcapsular segment 7 posteriorly (*arrow*). SS EPI DWI (b 800 s/mm2) (*B*) and corresponding ADC map (*C*) demonstrate intralesional restricted diffusion. Axial noncontrast GRE T1WI (*D*), and arterial (*E*), portal venous (*F*), and transitional (*G*) postcontrast phases demonstrate a hypointense mass in segment 7 (*arrows*) with subtle rim arterial phase hyperenhancement and progressive delayed internal enhancement. The lesion is hypointense in the hepatobiliary phase (*H*). Pathology at percutaneous biopsy was consistent with hepatocellular carcinoma.

Cystic hepatocellular carcinoma

HCC that undergoes internal necrosis, cystic degeneration, or hemorrhage can present as a multilocular cystic mass.[20] Cystic HCC is a rare entity generally seen in rapidly growing tumors.[21] Cross-sectional imaging findings that help differentiate cystic HCC from other cystic neoplasms (ie, mucinous cystic neoplasm and metastases) or benign cystic lesions (ie, hepatic abscess, echinococcal cyst, intrahepatic hematoma, and biloma) include the presence of liver cirrhosis, typical imaging characteristics of HCC within the solid components, and vascular invasion.[19,20] Compared with simple fluid, the attenuation of the cystic component of HCC is similar or slightly higher density on CT and has slightly hypointense signal intensity on T2-weighted MRI.[20] Clinical history can help distinguish cystic HCC from HCC treated with locoregional therapies with subsequent liquefactive necrosis, which can appear cystic on cross-sectional imaging.[22]

Fibrolamellar hepatocellular carcinoma

Fibrolamellar HCC mainly occurs in young adults (average age 25 years) without underlying liver disease.[23] These are classically large, well-defined (80%–100%), lobulated tumors with internal heterogeneity that can lead to a variable cross-sectional imaging appearance.[23] Fibrolamellar HCC is typically hypodense on noncontrast CT, and most (approximately 90%) demonstrate heterogeneous APHE. The lesion has a widely variable appearance on PVP CT: 48% of lesions are isodense, 16% are hyperdense, and 36% are hypodense relative to the liver. A central stellate scar is observed in 71% of the lesions. 68% of the scars contain calcifications and 95% of the scars are associated with radial septa.[23] Delayed enhancement of the scar is reported in 25% to 65% of lesions, however, should not be used as a distinguishing feature on CT as focal nodular hyperplasia (FNH) may also demonstrate delayed enhancement of the scar.[23,24]

On MRI, fibrolamellar HCC is typically T1 hypointense and T2 hyperintense, with heterogeneous enhancement on the arterial phase that becomes isointense or hypointense on the PVP and DP following contrast administration.[24] MRI may have an advantage for the characterization of the central scar, as the central scar within fibrolamellar HCC is typically T1 and T2 hypointense, compared

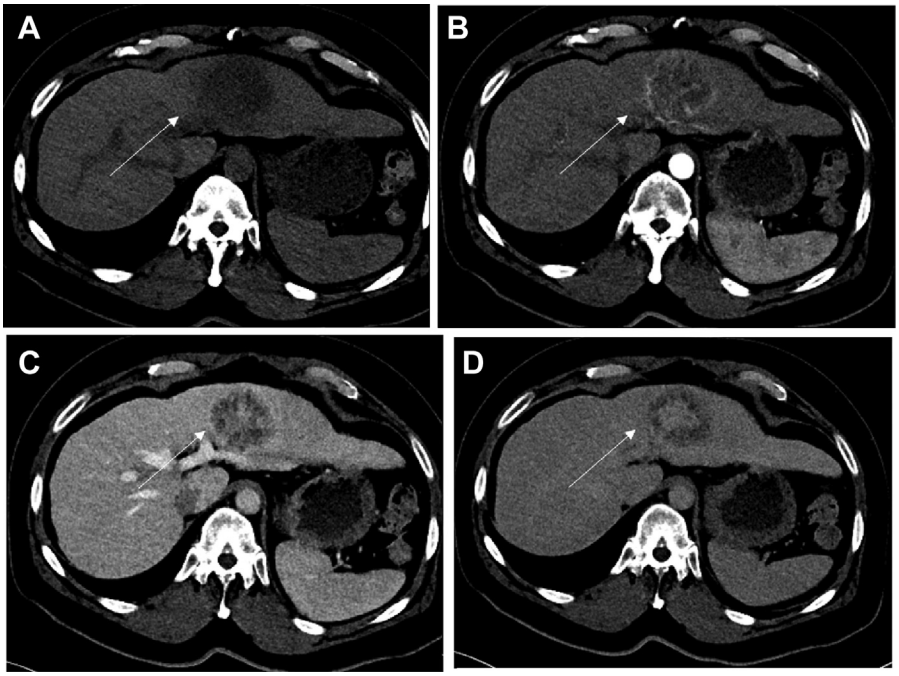

Fig. 3. 69-year-old woman with cirrhosis and incidental liver mass. Axial noncontrast CT (*A*) demonstrates a well-defined hypoattenuating mass in segment 2 (*arrow*). Postcontrast arterial phase (*B*), portal venous phase (*C*), and transitional phase (*D*) axial CTs demonstrate rim arterial phase hyperenhancement, central progressive enhancement, and delayed peripheral washout. Pathology at percutaneous biopsy demonstrated poorly differentiated carcinoma, with hepatocellular carcinoma favored over cholangiocarcinoma.

with the scar in FNH which is typically T2 hyperintense. Additionally, fibrolamellar HCC does not typically retain hepatobiliary specific contrast agents, which helps to differentiate it from FNH (**Fig. 5**).[24]

Combined hepatocellular carcinoma/intrahepatic cholangiocarcinoma

Combined hepatocellular carcinoma-cholangiocarcinoma (cHCC-ICC) is a rare primary liver tumor that demonstrates imaging and histologic features of both HCC and ICC.[25] Given the rarity of this entity, many of its clinical and demographic features, prognostic factors and optimal treatment options remain poorly understood.[26] The preoperative diagnosis of cHCC-ICC is important as patients can proceed to transplant without histology; however, significant overlap of HCC and ICC imaging features and inherent tumor heterogeneity make this quite difficult.[27] Previous studies have reported that imaging features of cHCC-ICC more closely resemble ICC and metastasis rather than HCC; however, a recent study of 61 cHCC-ICCs demonstrated that 54.1% of the lesions met LI-RADS criteria for HCC, and therefore might have originally been misclassified.[28–34]

cHCC-ICC generally appears as a hypodense or isodense mass on noncontrast CT and as a T1 hypointense, T2 intermediate or hyperintense mass on MRI.[35] Diffusion restriction, intralesional fat, hemorrhage, biliary obstruction, tumor thrombus, and/or overlying capsular retraction may be visualized, lending to its individual HCC and ICC components.[27] The enhancement pattern on CT and MRI can also be quite variable, with most cHCC-ICC lesions demonstrating whole-lesion or rim APHE, either with progressive central enhancement, central or peripheral washout, or washout and progression on more delayed phases (**Fig. 6**).[27,31] The presence of washout, washout and progression, intralesional fat, and hemorrhage were all strongly associated with cHCC-ICC when directly compared with ICC.[27]

Biliary Duct Origin

Intraductal papillary neoplasm of the bile duct

Intraductal papillary neoplasm of the bile duct (IPN-B) is analogous to the intraductal

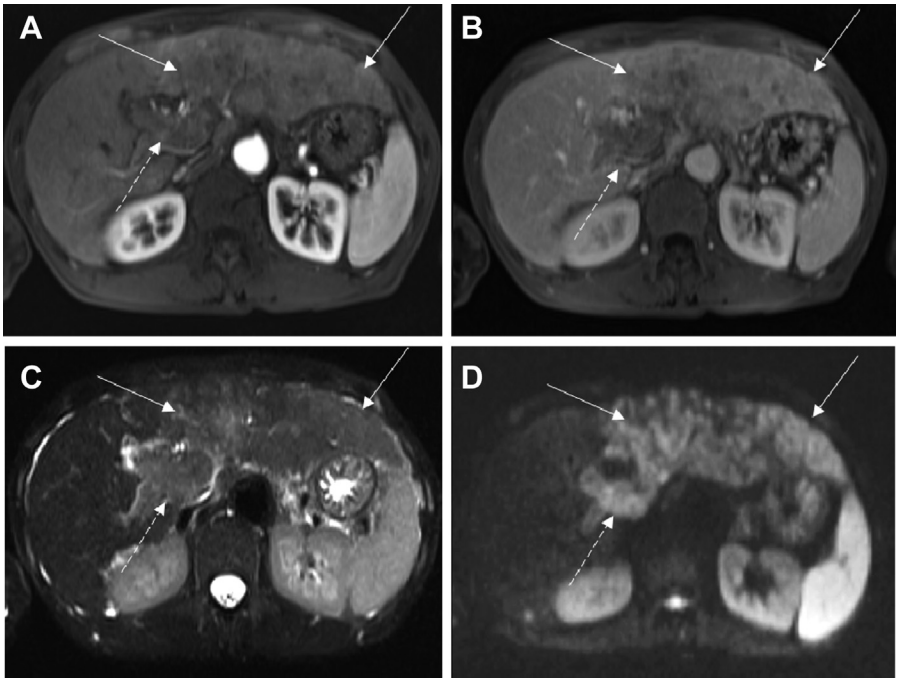

Fig. 4. 57-year-old man with elevated alpha-fetoprotein (AFP) of 544.9 ng/mL and infiltrative HCC. Axial postcontrast GRE T1WI during the arterial phase (*A*) demonstrates heterogenous enhancement in the left lobe, with ill-defined discrete and confluent hypointense nodules on portal venous phase (*arrows*) (*B*). Axial T2 FSE with fat saturation (*C*) and SS EPI DWI (b 800 s/mm2) demonstrate corresponding diffuse and heterogeneous signal hyperintensity in the left lobe, consistent with infiltrative HCC (*arrows*). Expansion of the portal vein with heterogeneous enhancement and T2/DWI hyperintensity are also present, consistent with tumor thrombus (*dashed arrows*).

papillary mucinous neoplasm of the pancreas (IPMN) given that they share similar embryologic, clinical, and histopathologic features.[36,37] Typical clinical presentation involves symptoms related to biliary obstruction by tumor and/or thick intraductal mucin, including abdominal pain, jaundice, elevated liver enzymes, and cholangitis.[38]

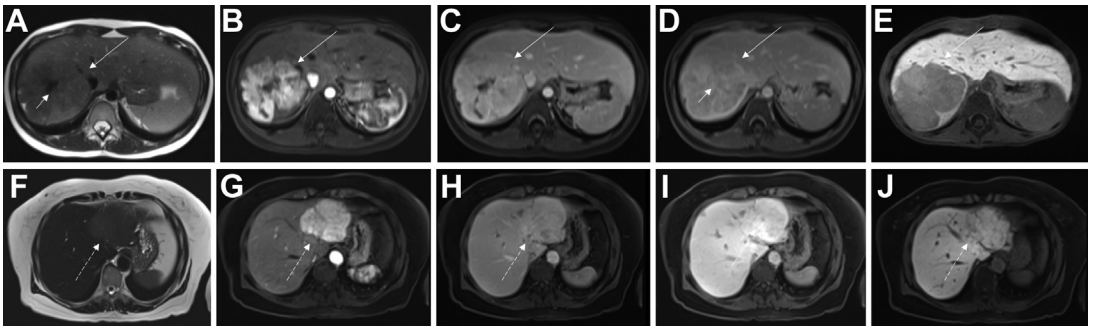

Fig. 5. Similar and contrasting imaging characteristics of fibrolamellar hepatocellular carcinoma (HCC) compared with focal nodular hyperplasia (FNH). Contrast-enhanced MRI using an extracellular contrast agent in a 15-year-old woman with an incidental liver mass reveals a 10.0 cm mildly T2 hyperintense solid mass in segments 7 and 8 (*arrow*) (*A*) with arterial phase hyperenhancement (APHE) (*B*) and no portal venous or equilibrium phase washout (*C*, *D*). Delayed enhancement of the T2 hypointense central scar is present (short *arrow*). Subsequent MRI with gadoxetic acid-enhanced MRI demonstrates delayed hepatobiliary phase (HBP) hypointensity (*E*). Pathology revealed fibrolamellar HCC. Similar mild T2 hyperintensity and dynamic postcontrast imaging findings are noted in an 8.3 cm solid mass in segments 2 and 3 in a 65-year-old woman (*dashed arrow*) (F through I) on gadoxetic acid-enhanced MRI. Delayed HBP (*J*) in this patient reveals hyperintensity in the lesion, diagnostic for FNH. No central scar was identified in the FNH.

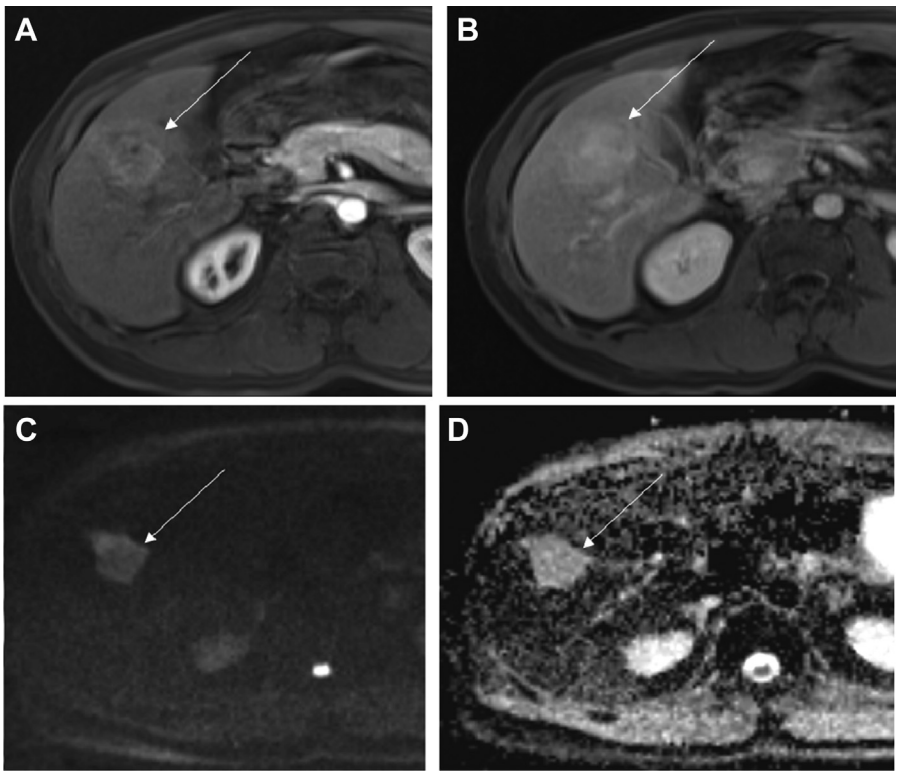

Fig. 6. 46-year-old man with chronic hepatitis B, elevated AFP (44.8 ng/mL), and new liver mass on prior screening ultrasound. Axial GRE T1WI demonstrates a peripherally enhancing mass in segment 5 on the arterial phase (*A*) with progressive whole-lesion enhancement in the portal venous phase (*B*) SS EPI DWI (b 800 s/mm2) (*C*) and corresponding ADC map (*D*) demonstrate intralesional restricted diffusion, imaging features that are typical for intrahepatic cholangiocarcinoma (ICC). This patient had a normal CA 19-9 level. Pathology at resection demonstrated cHCC-ICC.

Macroscopically, IPN-B appears as a papillary lesion within a bile duct lumen, with varying degrees of associated mucin production (mucin is detected macroscopically in approximately 1/3 of cases of IPN-B).[39] As the lesion spreads along the bile duct mucosa, multiple lesions can be seen in up to 50% of cases.[40] Surgical resection is considered the treatment of choice as the lesion may demonstrate an invasive component; accurate preoperative diagnosis is, therefore, critical as the lesion is approached surgically similar to a cholangiocarcinoma.[41–43]

Four different imaging manifestations have been described, primarily related to the balance between papillary proliferation and mucin production: (1) mass with proximal duct dilatation; (2) disproportionate duct dilatation without mass; (3) mass with proximal and distal duct dilatation (most common subtype); and (4) cyst forming.[44] When IPN-B is associated with abundant mucin production, it may cause dilatation of the bile duct distal to the lesion, which is considered a characteristic feature.[45] In the cystic subtype, internal papillary projections may be visible, and communication between the cystic mass and bile duct is often a clue to differentiate between other cystic hepatic lesions.[46]

On CT, the lesion appears as an intraductal mass that is generally iso- or hyperattenuating to surrounding liver.[47] On MRI, it is T1 iso- or hypointense to surrounding liver and appears as a papillary filling defect within a dilated bile duct on T2-weighted images. Following contrast administration, the lesion demonstrates iso- or mild hyperintensity on the late arterial phase but does not remain hyperintense during the PVP or DP, unlike intraductal cholangiocarcinoma which shows progressive PVP and DP enhancement.[48] Diffusion restriction may be present within any solid components. Mucin may appear as linear filling defects on hepatobiliary phase MRI or MRCP.[49,50] Malignant components can be found in 31% to 83% of cases of IPN-B, which, in addition to the above-described features, would also show avidity on FDG-PET and macroscopic peribiliary enhancement.[43,48,51]

Mucinous cystic neoplasms with invasive features

Previously referred to as biliary cystadenomas, mucinous cystic neoplasms (MCN) are biliary neoplasms composed of mucin-producing epithelium.[52,53] There is a reported 20% risk of malignant transformation to invasive MCN(formerly referred to as biliary cystadenocarcinoma).[53] Although widely reported as occurring almost exclusively in females—theorized to be secondary to the essential feature of ovarian-like subepithelial stroma—MCN has been reported in a small subset of male patients, typically in the fifth decade of life.[54,55] Clinical presentation is widely variable, with patients either being asymptomatic or presenting with right upper quadrant/epigastric pain, abdominal fullness, and/or a palpable abdominal mass.[56]

MCN is a very rare entity, with most published literature consisting of limited single-center studies or case reports. There are currently no well-established imaging features that differentiate noninvasive MCN from invasive MCN, and MCNs are usually resected to reliably identify their degree of malignancy.[55–57] The typical appearance of MCN on both CT and MRI is a large unilocular or multilocular cystic mass with enhancement and/or calcification of the septa, with or without visible mural nodules (**Fig. 7**). MCNs typically do not communicate with an adjacent bile duct, a key differentiating factor from cyst-forming IPN-B.[58] Adjacent ductal dilatation is, therefore, less commonly associated with MCN than IPN-B, and downstream ductal dilatation to the tumor is rarely observed.[58] Recent studies have demonstrated septal enhancement and septations arising from the cyst wall without an overlying indentation as highly sensitive features of MCN on CT and MRI.[53,59] In a subset comparison of noninvasive and invasive MCNs, a mural nodule, calcification, bile duct dilation, and intra-cystic debris were all characteristics of invasive MCNs.[60]

Mucinous cholangiocarcinoma

Mucinous cholangiocarcinoma (mCCA) is an extremely rare variant of ICC, with nearly all published literature on this entity consisting of case reports. Given the lesion's abundant mucin production, differentiation from other mucin-producing lesions (such as invasive IPN-B, invasive MCN, or mucinous metastasis) is prudent but remains extremely difficult.[61]

mCCA generally appears as a large, irregular, lobulated mass that may be almost entirely cystic or mixed solid/cystic, depending on the degree of mucin production (**Fig. 8**). Intra-tumoral calcification and portal vein tumor thrombus have been described. On CT, mCCA is generally hypodense, and solid components are hypovascular with peripheral enhancement following contrast administration, lending to possible confusion with hemangioma. On MRI, it is generally T1 hypointense and T2 hyperintense, and luminal communication between the tumor and bile duct on MRCP sequences may be observed.[61–63] Like the more common mass-forming ICC, upstream biliary obstruction, satellite nodules, adjacent hepatic perfusion anomaly, and parenchymal atrophy may be observed in mCCA.[64]

Neuroendocrine origin

Although mainly occurring in organs of the bronchopulmonary or gastrointestinal tract, primary neuroendocrine tumors (NETs) can occur in almost any organ.[65] Primary hepatic neuroendocrine tumor (PHNET), representing approximately 0.3% of all neuroendocrine tumors, is an extremely rare entity that is difficult to distinguish from the much more common metastatic hepatic NET, with fewer than 200 cases of PHNET reported in the literature.[66,67]

The clinical presentation of PHNET is nonspecific and may include vague abdominal pain, jaundice, palpable right upper quadrant mass, weight loss, and diarrhea.[67] It has been reported that less than 20% of patients with PHNET present with classic carcinoid syndrome (described as skin flushing, abdominal pain, and episodic diarrhea).[68–70] Surgical resection is considered the mainstay of treatment, supplemented by systemic chemotherapy, radiation, and targeted locoregional and molecular therapies.[71]

The imaging appearance of PHNET is similar to metastatic hepatic NET. On CT, the lesion is typically a round, well-circumscribed, hypodense mass that demonstrates heterogeneous APHE following contrast administration. Calcification and/or internal heterogeneity/necrosis are rare yet may become more frequent as tumors grow larger.[71] On MRI, the lesion is generally a round, well-circumscribed, T1 hypointense, T2 hyperintense mass with APHE, DP capsule, HBP hypointensity, and diffusion restriction.[67,72] They can demonstrate radiotracer avidity on both FDG and somatostatin receptor analog (eg, gallium-68 DOTATATE) PET.[73]

PRIMARY HEPATIC SARCOMAS

Angiosarcoma

Although primary hepatic angiosarcoma accounts for only 2% of primary hepatic tumors, it is the most common hepatic malignancy of mesenchymal origin. This tumor demonstrates a strong

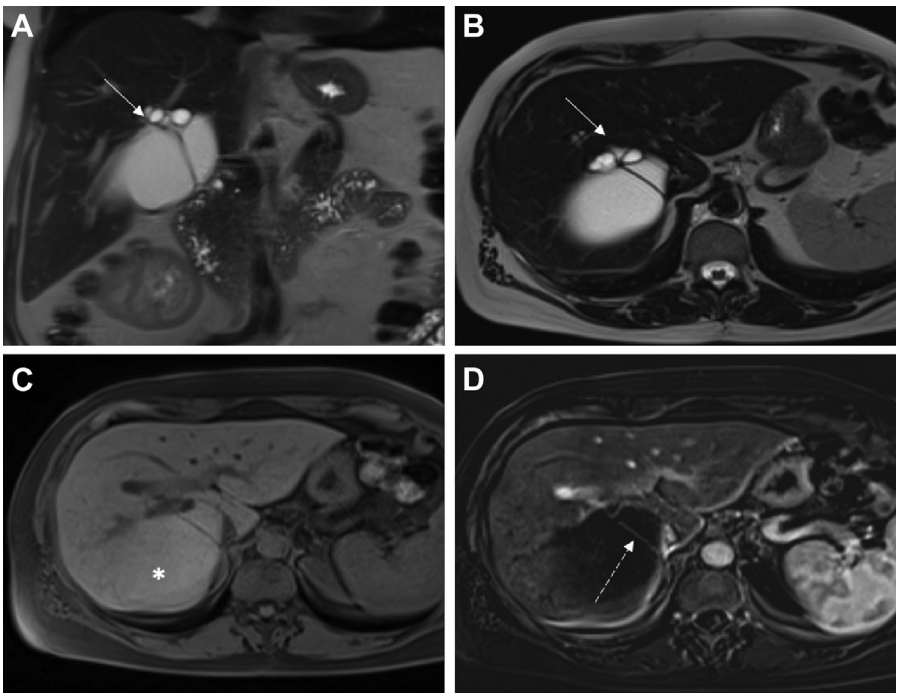

Fig. 7. 51-year-old woman with a multiloculated mucinous cystic neoplasm of the liver. Coronal (*A*) and axial (*B*) SS FSE T2WI demonstrate an 11.0 cm multiloculated cystic mass containing thin septations (*arrows*). On axial noncontrast GRE T1WI (*C*), the largest cystic component contains T1 hyperintense material, consistent with mucin (*asterisk*). Thin perceptible septal enhancement is present in the portal venous phase subtracted GRE T1WI (*dashed arrow*) (*D*). Pathologic diagnosis of multiloculated mucinous cystic neoplasm was confirmed given the presence of simple cuboidal epithelium with underlying "ovarian-like" cellular stroma that was positive for estrogen and progesterone receptors by immunohistochemistry stains following partial hepatectomy.

male predominance, and most commonly presents in the clinical setting of hematologic abnormalities, such as anemia and thrombocytopenia. Exposure to environmental carcinogens, including thorium dioxide (Thorotrast), arsenic, and vinyl chloride has previously been associated with hepatic angiosarcoma; however, exposure to these substances is now uncommon. Moreover, many cases now are reported in the absence of known risk factors.[74]

The diagnosis of hepatic angiosarcoma is often challenging due to the known vascularity and pleomorphic histopathology of this tumor, which result in both an increased risk of hemorrhage with biopsy and a varied spectrum of imaging appearances, respectively.[75] Reported CT findings include multiple small nodules, a large dominant mass, a mixed presentation with a dominant mass and multiple nodules, or diffusely infiltrating tumor.[74] Furthermore, on CT, many of these small nodular lesions are hypodense compared with the normal hepatic parenchyma on both noncontrast and AP, with some cases demonstrating mild hyperenhancement on AP.[74,75] Though often confused with benign hepatic hemangioma, multiple recent reports have shown the enhancement pattern of hepatic angiosarcoma to vary from hemangioma in multiple ways.[16,74,75] In contrast to the characteristic progressive, nodular, discontinuous centripetal enhancement of hemangiomas, angiosarcomas demonstrate irregular central and rim enhancement of a lower attenuation than that of the aorta.[74] On MRI, larger dominant masses are typically heterogeneous and T2 hyperintense, with or without T1 hyperintense hemorrhagic components and/or fluid-fluid levels representing intra-tumoral necrosis. Postcontrast MRI demonstrates heterogeneous AP and PVP enhancement with progressive enhancement on DP, barring regions of internal necrosis, fibrosis, or hemorrhage (**Fig. 9**).[74,75]

Given the highly variable appearance of angiosarcoma, including overall lesion appearance and enhancement pattern, differential diagnostic considerations include HCC, ICC, and hypovascular and hypervascular metastases. Apart from distinguishing clinical and laboratory features, the progressive enhancement on delayed imaging of angiosarcoma is significant, as it would be atypical of HCC. In addition, periductal enhancement and

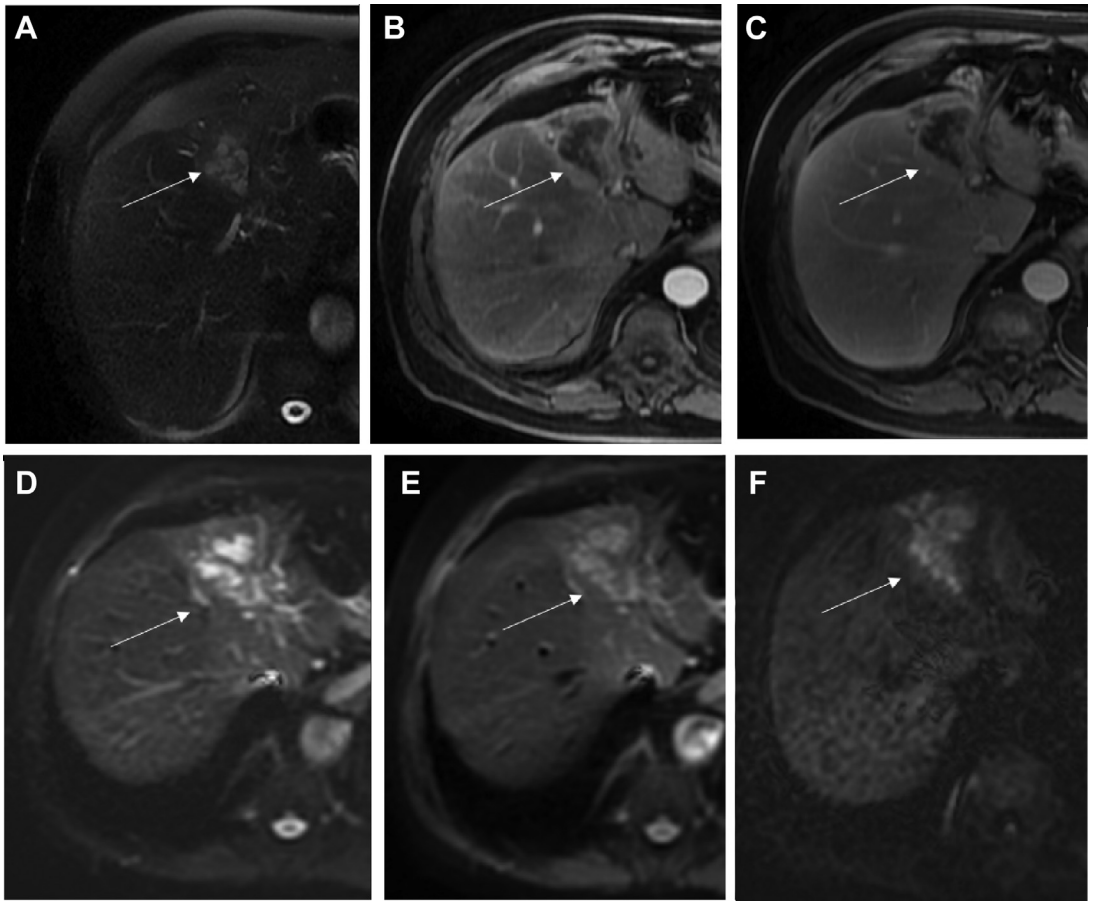

Fig. 8. 73-year-old man with new liver mass. Axial T2 FSE with fat saturation (*A*) axial GRE T1WI with arterial (*B*) and portal venous phases (*C*) and SS EPI DWI with b values of 10 s/mm2 (*D*) 500 s/mm2 (*E*) and 800 s/mm2 (*F*) demonstrate a 5.6 cm lobulated mass in segment 4A (*arrows*) with central areas of marked T2 hyperintensity. The lesion demonstrates minimal peripheral enhancement, surrounding biliary distention, and diffusion restriction. There is severe atrophy of the left lateral segment and perfusion anomaly surrounding the mass. Pathology at resection was consistent with mucinous cholangiocarcinoma.

intrahepatic biliary dilatation are findings that would favor cholangiocarcinoma.[74,76,77]

Hepatic Epithelioid Hemangioendothelioma

Hepatic epithelioid hemangioendothelioma (HEHE) is a rare and low-grade malignant tumor of vascular origin with an increased female predominance. Approximately 36% of patients demonstrate extra-hepatic lesions at diagnosis, most commonly within the lungs, lymph nodes, and peritoneum. Accurate diagnosis is essential as HEHE can often be treated with surgical resection or transplantation regardless of the presence of metastatic disease. However, diagnosis remains challenging due to the variable clinical presentation and the range of potential imaging appearances.[76,78]

Most cases of HEHE demonstrate multifocal and peripherally distributed or subcapsular lesions, which ultimately increase in size and coalesce to form larger confluent masses.[76,78] Capsular retraction and hypertrophy of the normal hepatic parenchyma have been reported. The most common cross-sectional imaging appearance is multifocal low-density hepatic nodules of varying sizes (**Fig. 10**). Earlier stage disease, as mentioned above, demonstrates a multifocal and peripheral nodular pattern, while more progressed forms have confluent masses. Associated calcification or central hypodensity on nonenhanced CT images, possibly reflecting central necrosis, are also described. Postcontrast CT images demonstrated mild peripheral enhancement in some cases.[79] On MRI, lesions typically demonstrate T1 hypointensity with heterogeneous or

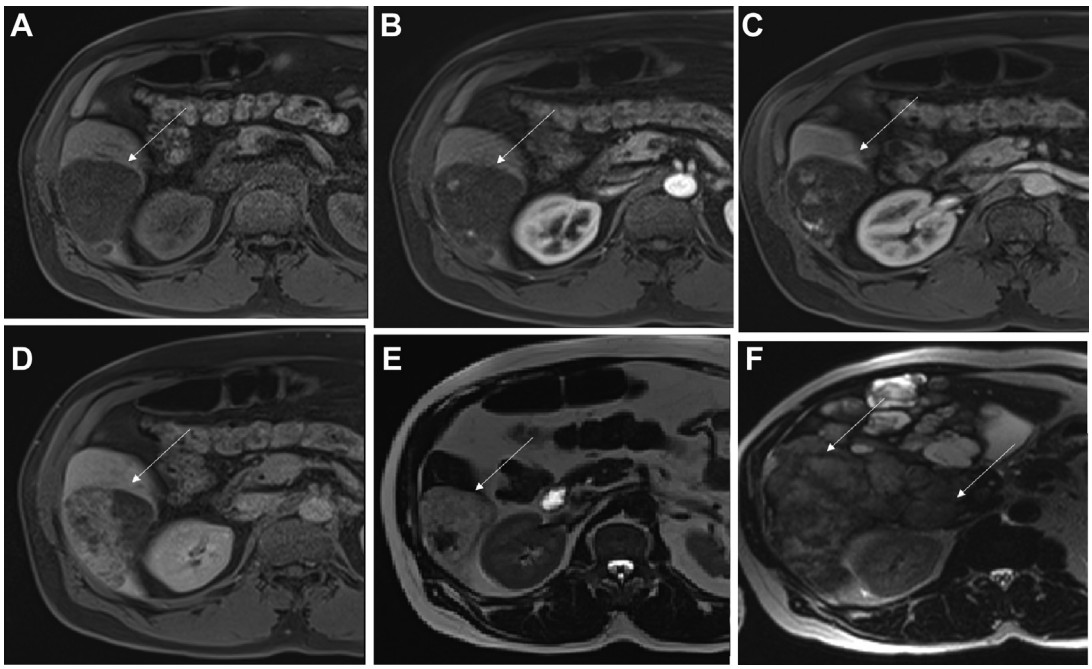

Fig. 9. 57-year-old man with hepatic epitheloid angiosarcoma. Axial noncontrast GRE T1WI (*A*) and arterial (*B*) portal venous (*C*) and transitional (*D*) postcontrast phases demonstrate a dominant hypointense mass in segment 6 (*arrows*) with progressive heterogeneous internal enhancement. No significant hemorrhage or necrosis was identified in the lesion. Three-month follow-up axial SS FSE T2WI (*E-F*) demonstrates significant tumor progression.

targetoid T2 hyperintensity. Most lesions also demonstrate immediate peripheral enhancement on postcontrast sequences. Delayed postcontrast sequences showed progressive central filling in some cases. The differential diagnosis is quite extensive, including hemangiomas, abscesses, FNH, HCC, and metastases.

The lollipop sign is an imaging sign that has been reported to increase the specificity and recognition of HEHE on cross-sectional imaging.[78,79] The lollipop sign has two components, the first being the round, well-circumscribed hypodense tumor, most commonly with an avascular core (the candy), and the second being an adjacent histologically occluded vein (the stick). Additional reported but uncommon imaging characteristics include cavitating or complex exophytic tumor, the presence of a central enhancing scar, or hyperenhancement of the lesion.[79,80]

Fibrosarcoma

Fibrosarcoma is a malignant tumor derived from fibroblasts and usually occurs in the limbs, head and neck, and the trunk, while rarely occurring in the viscera. According to Ito and colleagues from 1924 to 1990, only 33 cases of hepatic fibrosarcoma were reported in the literature.[81] Currently, diagnosis is made at pathology as there is no imaging finding characteristic for hepatic fibrosarcoma. Case reports have described lesions containing cystic degeneration and hemorrhage, portal vein involvement, or heterogeneous AP enhancement at CT.[82,83]

Leiomyosarcoma

Primary hepatic leiomyosarcoma is extremely rare, with probable origin from the smooth muscle cells of the hepatic veins or bile ducts. Most cases generally reflect metastases from extra-hepatic sites, including the gastrointestinal system, uterus, retroperitoneum, or lung. The tumor is most commonly found in middle-aged or older patients without a gender predisposition or a clear association with chronic hepatic disease or cirrhosis.[84] Interestingly, an increased number of cases of primary hepatic leiomyosarcoma in a younger population with human immunodeficiency virus (HIV) and in immunosuppressed transplant patients have recently been reported.[85]

The most frequently described finding is a large, well-circumscribed, and heterogeneously hypodense mass with internal enhancement on postcontrast CT. An appropriate clinical history is essential as additional studies have reported an

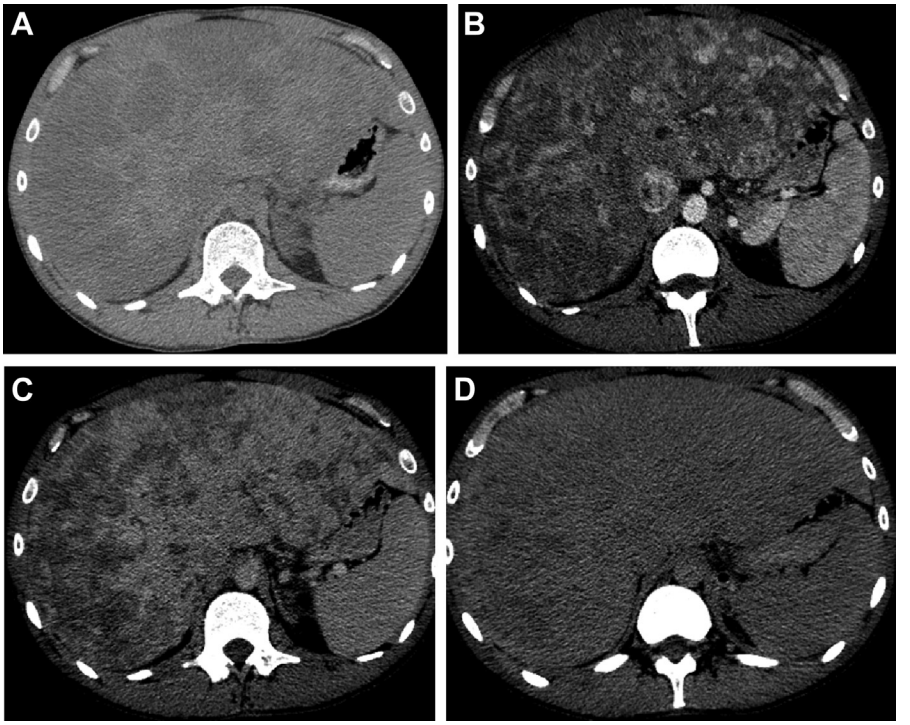

Fig. 10. 32-year-old man with epigastric pain and hepatic epithelioid hemangioendothelioma. Axial noncontrast CT (*A*) demonstrates extensive, confluent hypodense masses throughout both hepatic lobes. Postcontrast arterial phase (*B*) portal venous phase (*C*) and delayed phase (*D*) axial CTs demonstrate innumerable predominantly rim-enhancing lesions on the arterial phase with progressive central filling.

enhancing, thickened wall, which may mimic the findings of an abscess or hydatid cyst.[86] On MRI, these lesions generally demonstrate homogenous or heterogenous T1 signal, which may reflect internal hemorrhage, with associated high signal on T2-weighted sequences. Marked enhancement on the delayed postcontrast sequences is also generally noted without significant enhancement on arterial or venous phase.[83,87]

Kaposi Sarcoma

Kaposi sarcoma is a low-grade malignancy associated with human herpesvirus-8 (HHV-8) and is the most common intrahepatic neoplasm in patients with acquired immunodeficiency syndrome (AIDS). Less commonly, Kaposi sarcoma has also been reported in immunocompromised solid organ transplant recipients.[76]

Hepatic Kaposi sarcoma most commonly presents as multifocal parenchymal nodules, usually originating from the perivascular regions of the peripheral portal venous branches. Multiple hypoattenuating nodules in a perivascular and periportal distribution are noted on noncontrast CT. No significant associated enhancement is generally noted on AP or PVP, although there may be diffuse enhancement on DP.[76,88,89] Other differential diagnoses include metastatic lesions, fungal microabscesses, and multiple hemangiomas, for which associated Kaposi cutaneous involvement would be most helpful in narrowing the diagnosis.

Malignant Fibrous Histiocytosarcoma/ Histiocytoma

Although malignant fibrous histiocytosarcoma (MFH) is the most common soft tissue sarcoma in the adult population, involvement of the visceral organs, including the liver, is very rare.[90] Most cases occur in adults over the age of fifty with a slight male predominance. The complex internal architecture of these tumors, including hemorrhage, necrosis, myxoid degeneration, and/or fibrosis results in a large, heterogenous, and predominantly hypodense mass on noncontrast CT images with occasional involvement of the adjacent liver capsule. A spectrum of postenhancement appearances has been noted including a large heterogeneously enhancing mass with internal necrosis, a large mass with an enhancing peripheral pseudo-capsule, as well as a multiloculated cystic mass with progressively enhancing fibrotic internal septations. Despite

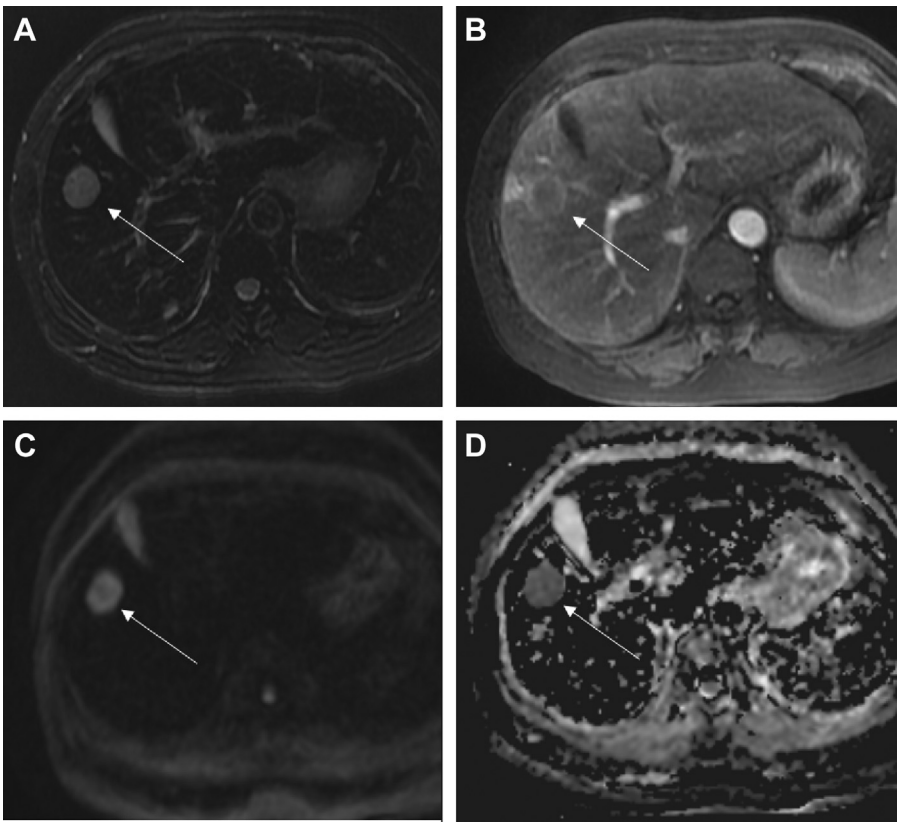

Fig. 11. 58-year-old woman with a history of allogeneic stem cell transplant for acute myeloid leukemia (AML) presenting with multiple liver lesions. Axial T2 FSE with fat saturation (*A*) demonstrates a 2.7 cm well-defined, T2 hyperintense mass in segment 5 (*arrow*). There is peripheral and mild central enhancement with surrounding shunting on portal venous phase GRE T1WI (*B*). Axial SS EPI DWI (b 800 s/mm2) (*C*) and corresponding ADC map (*D*) demonstrate intralesional diffusion restriction. Diffuse iron deposition is noted in the background liver, as evidenced by marked T2, DWI, and ADC hypointensity. Subsequent biopsy of this lesion revealed posttransplant lymphoproliferative disease (PTLD).

the rather aggressive appearance of hepatic MFH, there has been no report of bile duct obstruction, portal vein occlusion, or lymph node metastasis.[1]

Similarly, the few reported cases with MRI demonstrated a large, predominantly T1 hypointense and T2 hyperintense, lobulated mass with well-circumscribed margins and associated heterogenous and progressive enhancement. Although there is no distinctive imaging feature, hepatic MFH should be considered in a patient with an aggressive-appearing and large necrotic/cystic lesion of unknown etiology.[1,87,90]

HEMATOLOGIC ORIGIN

Primary Hepatic Lymphoma

Primary hepatic lymphoma (PHL) is a subset of non-Hodgkin lymphoma that is confined to the liver and perihepatic lymph nodes without distant involvement for at least 6 months after disease onset.[91] Although liver involvement is common in systemic lymphoma, PHL is exceedingly rare, accounting for less than 0.4% of extranodal lymphoma and is rising in incidence.[92] As the treatment of PHL consists primarily of combination chemotherapy, correct diagnosis is crucial and may spare the patient from surgical resection.

PHL is variable in appearance and most frequently presents as a solitary mass or multiple masses. A diffuse or infiltrative pattern is rare and confers a worse prognosis.[85] On CT, PHL presents as a solitary or multiple hypoattenuating masses, and may appear heterogeneous due to internal hemorrhage or necrosis. Calcification in untreated lesions is rare.[93] Following contrast administration, PHL may demonstrate minimal to no enhancement, patchy enhancement, or rim enhancement.[94] On MRI with liver-specific contrast agents, PHL is typically T1 hypointense, T2 hyperintense, and demonstrates hypointense

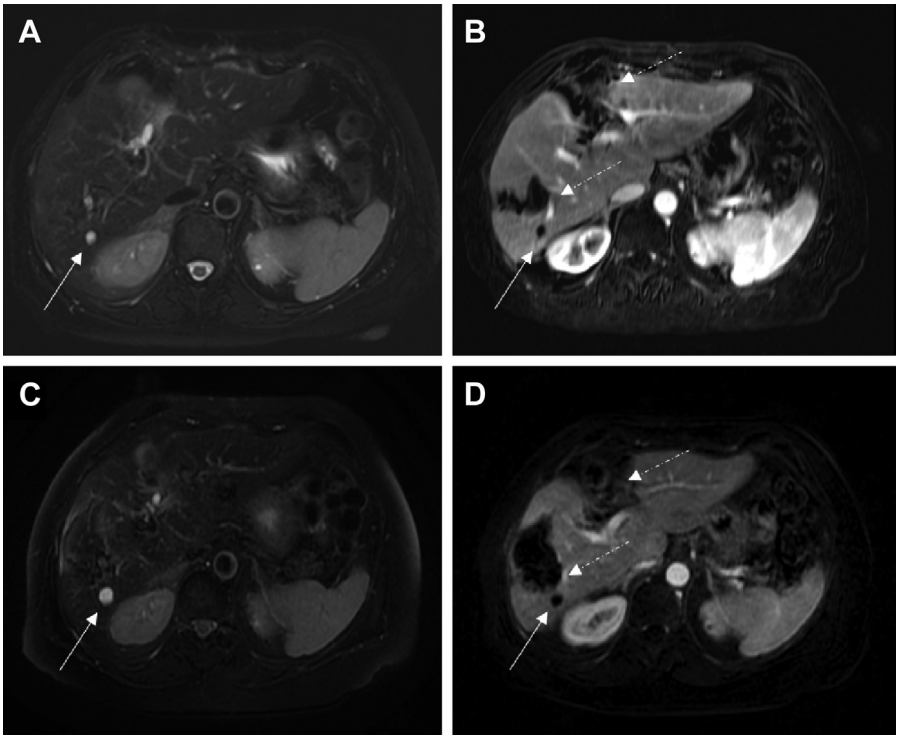

Fig. 12. 62-year-old woman with a history of cystic neuroendocrine liver metastases. Axial T2 FSE with fat saturation (*A*) demonstrates a 6 mm T2 hyperintense cyst in segment 6 (*arrow*) without enhancement on portal venous phase postcontrast GRE T1WI (*B*). The patient had previously undergone surgical wedge resection and ablation of other hepatic metastatic lesions in segments 4 and 6 (dashed *arrows*). Follow-up MRI 6 months later demonstrates interval enlargement of the segment 6 cystic lesion on axial T2 FSE with fat saturation (*C*) and subtracted portal venous phase postcontrast GRE T1WI (*D*), now measuring 12 mm.

signal on HBP.[95] Like other lymphomas, PHL demonstrates hyperintense signal on DWI with corresponding low ADC values reflective of their hypercellularity. Whole-body DWI has been shown to be comparable to FDG-PET/CT for the staging of lymphoma.[96]

Posttransplant Lymphoproliferative Disease

Posttransplant lymphoproliferative disease (PTLD) describes a spectrum of disease ranging from benign lymphoid hyperplasia to frank lymphoma following solid organ or hematopoietic stem cell transplant. It is associated with Epstein–Barr virus reactivation in the setting of immunosuppression.[97] The first-line treatment is a reduction in immunosuppression, while other treatment modalities include rituximab, chemotherapy, radiation, and/or antiviral therapy.[97] Extranodal disease is more common than nodal disease in PTLD, with the liver being the most involved abdominal solid organ.[98]

Hepatic involvement of PTLD may manifest (in descending order of frequency) as focal liver mass or masses, ill-defined infiltrative lesions, or as a porta hepatis mass, potentially causing hepatomegaly and biliary obstruction.[99] While vascular encasement may occur in PTLD, vessel invasion, thrombosis or occlusion is rare.[100] PTLD lesions are typically hypoattenuating with minimal to absent contrast enhancement on CT. On MRI, PTLD typically demonstrates hypointense signal on T1, mildly hyperintense signal on T2, with minimal to absent enhancement on postcontrast sequences (**Fig. 11**).[99] Similar to other lymphomas, PTLD demonstrates hyperintense signal on DWI with corresponding low ADC values, making whole-body DWI a potentially viable alternative to FDG-PET-CT for the diagnosis, staging, and assessment of treatment response in patients with PTLD.[96,101]

METASTATIC DISEASE

Due in part to its dual vascular supply, the liver is one of the most frequent sites of metastasis. A study by Horn and colleagues using data from the Surveillance, Epidemiology, and End Results (SEER) database found that 5.1% of patients

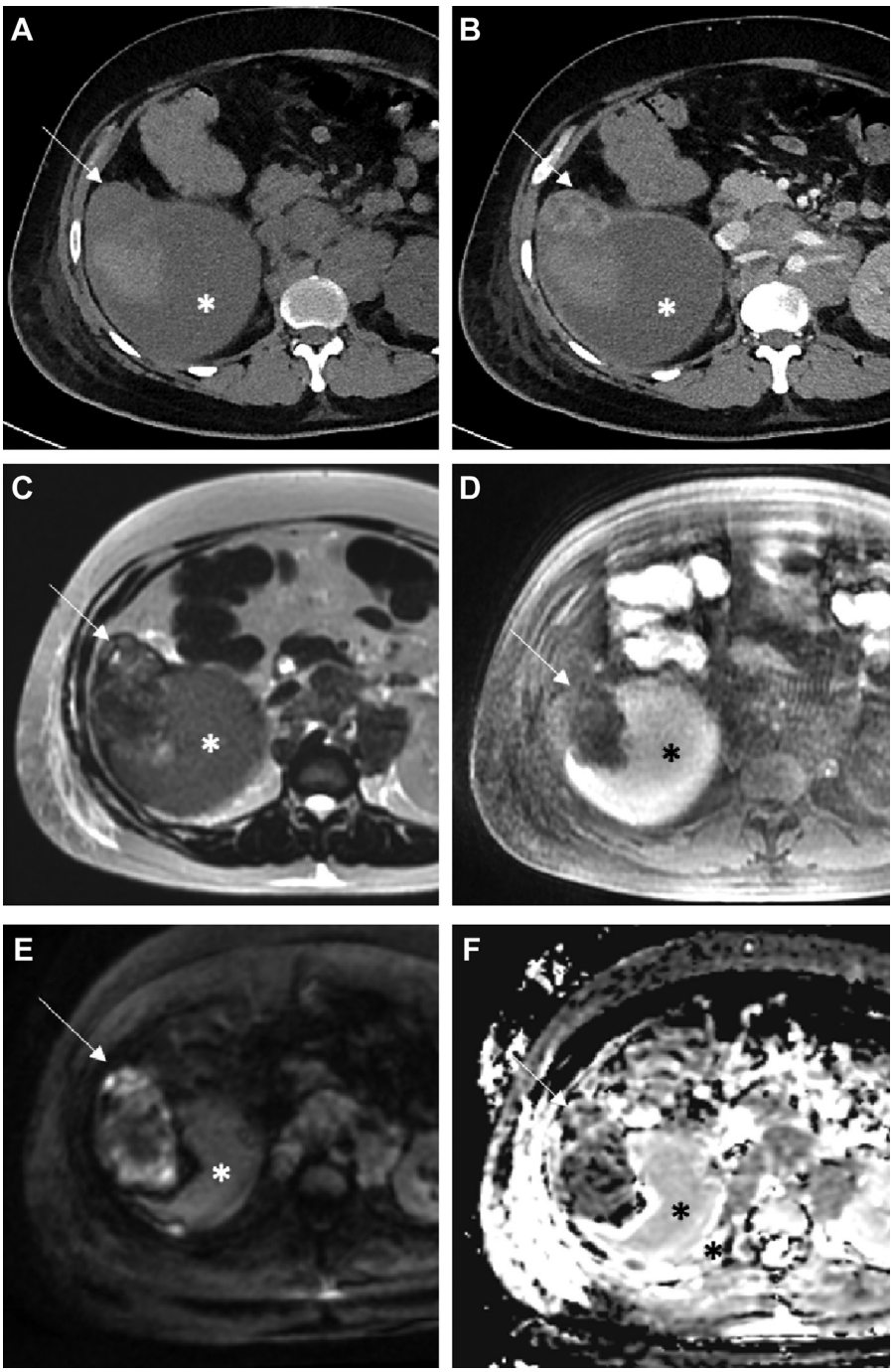

Fig. 13. 35-year-old man with hemorrhagic liver metastases from gastroesophageal junction adenocarcinoma. Pre (*A*) and postcontrast (*B*) axial CTs demonstrate a complex cystic-solid mass in hepatic segments 5/6, with a 4.0 cm enhancing component along the anterior margin (*arrows*) and a complex predominantly low attenuation cystic component posteriorly (*asterisk*). MRI was then performed for further characterization, revealing T2 intermediate (*C*) and T1 hyperintense (*D*) material in the posterior component, most consistent with hemorrhage (*asterisk*). Axial SS EPI DWI (b 800 s/mm2) (*E*) and corresponding ADC map (*F*) demonstrate intralesional restricted diffusion. Metastatic retroperitoneal lymphadenopathy is also noted.

have synchronous liver metastasis at the time of primary cancer diagnosis and that survival for patients with liver metastasis was significantly decreased compared with patients without liver metastasis.[102] The imaging features of hepatic metastases are highly variable and often depend on histology of the primary malignancy; however, atypical features include cystic components and hemorrhage, which are discussed herein.

Cystic Hepatic Metastases

Liver metastases may be cystic due to high mucin content reflective of the primary tumor, such as in ovarian cystadenocarcinoma or colorectal adenocarcinoma. Alternatively, the cystic component may be secondary to necrosis in metastasis that has been treated or has outgrown its blood supply. In general, cystic metastases have ill-defined borders, irregular walls, and demonstrate early arterial rim enhancement on CT and MRI.[103] On occasion, these metastases may be purely cystic (**Fig. 12**). The differential diagnosis includes polycystic liver disease, biliary hamartomas, abscesses, cystic HCC, and MCN or invasive MCN.[104]

Hemorrhagic Hepatic Metastases

Both hypervascular and hypovascular liver metastases have been reported to cause hepatic hemorrhage. However, hemoperitoneum is more frequently seen in association with primary liver tumors compared with liver metastases due to the higher degree of vascularity in primary liver tumors.[105] The hemorrhage may be contained or may rupture into the peritoneal space and potentially cause hemorrhagic shock and intraperitoneal tumor spillage. In the acute phase, hemorrhagic hepatic metastases are typically hyperattenuating on noncontrast CT and gradually decrease in attenuation over time. The MRI appearance of hemorrhagic hepatic metastases is highly variable depending on the age of the blood products (**Fig. 13**). The differential diagnosis includes hemorrhage into benign lesions (ie, hepatocellular adenoma) or primary liver malignancy (ie, HCC), rupture of a hepatic artery aneurysm, and spontaneous hepatic rupture in patients at risk for bleeding complications.[106]

SUMMARY

Atypical liver malignancies, which may be defined as either an atypical appearance of commonly encountered lesions or lesions that are encountered rarely, may present with a myriad of imaging appearances. Such variability at imaging poses a diagnostic challenge for the radiologist. Ultimately, knowledge of the patient's clinical history, laboratory values, pertinent imaging findings, as well as discussion in a multi-disciplinary setting, may enable an accurate diagnosis noninvasively. In this review, we sought to summarize the key CT and MRI findings in the context of clinical information for such liver lesions. The radiologist's enhanced knowledge of atypical liver malignancies will help achieve accurate diagnosis, and thus improved clinical treatment planning and patient care.

CLINICS CARE POINTS

- Liver malignancies result from the development of tumor from variety of cells in the liver (hepatocytes, biliary epithelium, hepatocytes, lymphocytes, neuroendocrine cells, et cetera) and secondarily from spread to the liver from other sites (metastatic disease).
- Certain tumors may have a characteristic appearance on cross sectional imaging, while certain tumors can be highly variable in appearance.
- The diagnostic radiologist's knowledge of atypical liver malignancies and unusual presentations of more common liver malignancies can aid the multidisciplinary clinical team in reaching the correct diagnosis and enabling appropriate management for the patient.
- Careful attention to imaging protocols and awareness of certain technical pitfalls can help in avoiding imaging misinterpretation.

DISCLOSURE

The authors have nothing to disclose.

REFERENCES

1. Tan Y, Xiao EH. Rare hepatic malignant tumors: dynamic CT, MRI, and clinicopathologic features: with analysis of 54 cases and review of the literature. Abdom Imaging 2013;38(3):511–26.
2. Kim JH, Joo I, Lee JM. Atypical appearance of hepatocellular carcinoma and its mimickers: how to solve challenging cases using gadoxetic acid-enhanced liver magnetic resonance imaging. Korean J Radiol 2019;20(7):1019–41.
3. Lewis S, et al. Volumetric quantitative histogram analysis using diffusion-weighted magnetic resonance imaging to differentiate HCC from other primary liver cancers. Abdom Radiol (NY) 2019;44(3):912–22.

4. Siegelman ES, Chauhan A. MR characterization of focal liver lesions: pearls and pitfalls. Magn Reson Imaging Clin N Am 2014;22(3):295–313.
5. Donato H, et al. Liver MRI: From basic protocol to advanced techniques. Eur J Radiol 2017;93:30–9.
6. Kartalis N, Brehmer K, Loizou L. Multi-detector CT: Liver protocol and recent developments. Eur J Radiol 2017;97:101–9.
7. Erkan B, et al. Non-invasive diagnostic criteria of hepatocellular carcinoma: Comparison of diagnostic accuracy of updated LI-RADS with clinical practice guidelines of OPTN-UNOS, AASLD, NCCN, EASL-EORTC, and KLSCG-NCC. PLoS One 2019;14(12):e0226291.
8. Chernyak V, et al. Use of gadoxetate disodium in patients with chronic liver disease and its implications for liver imaging reporting and data system (LI-RADS). J Magn Reson Imaging 2019;49(5):1236–52.
9. Aslam A, et al. Assessing locoregional treatment response to Hepatocellular Carcinoma: comparison of hepatobiliary contrast agents to extracellular contrast agents. Abdom Radiol (NY) 2021;46(8):3565–78.
10. Wile GE, Leyendecker JR. Magnetic resonance imaging of the liver: sequence optimization and artifacts. Magn Reson Imaging Clin N Am 2010;18(3):525–547, xi.
11. Marin D, et al. State of the art: dual-energy CT of the abdomen. Radiology 2014;271(2):327–42.
12. Karcaaltincaba M, Akhan O. Imaging of hepatic steatosis and fatty sparing. Eur J Radiol 2007;61(1):33–43.
13. Kovac JD, et al. An overview of hepatocellular carcinoma with atypical enhancement pattern: spectrum of magnetic resonance imaging findings with pathologic correlation. Radiol Oncol 2021;55(2):130–43.
14. Leoni S, et al. The impact of vascular and nonvascular findings on the noninvasive diagnosis of small hepatocellular carcinoma based on the EASL and AASLD criteria. Am J Gastroenterol 2010;105(3):599–609.
15. Choi JW, et al. Hepatocellular carcinoma: imaging patterns on gadoxetic acid-enhanced MR Images and their value as an imaging biomarker. Radiology 2013;267(3):776–86.
16. White PG, Adams H, Smith PM. The computed tomographic appearances of angiosarcoma of the liver. Clin Radiol 1993;48(5):321–5.
17. Renzulli M, Golfieri R, Bologna Liver Oncology Group. Proposal of a new diagnostic algorithm for hepatocellular carcinoma based on the Japanese guidelines but adapted to the Western world for patients under surveillance for chronic liver disease. J Gastroenterol Hepatol 2016;31(1):69–80.
18. Reynolds AR, et al. Infiltrative hepatocellular carcinoma: what radiologists need to know. Radiographics 2015;35(2):371–86.
19. Zhou X, et al. Hepatocellular carcinoma with hilar bile duct tumor thrombus versus hilar Cholangiocarcinoma on enhanced computed tomography: a diagnostic challenge. BMC Cancer 2020;20(1):54.
20. Qian LJ, et al. Spectrum of multilocular cystic hepatic lesions: CT and MR imaging findings with pathologic correlation. Radiographics 2013;33(5):1419–33.
21. Vachha B, et al. Cystic lesions of the liver. AJR Am J Roentgenol 2011;196(4):W355–66.
22. Abraham SC, et al. Histologic abnormalities are common in protocol liver allograft biopsies from patients with normal liver function tests. Am J Surg Pathol 2008;32(7):965–73.
23. Ichikawa T, et al. Fibrolamellar hepatocellular carcinoma: imaging and pathologic findings in 31 recent cases. Radiology 1999;213(2):352–61.
24. Ganeshan D, et al. Imaging features of fibrolamellar hepatocellular carcinoma. AJR Am J Roentgenol 2014;202(3):544–52.
25. Yin X, et al. Combined hepatocellular carcinoma and cholangiocarcinoma: clinical features, treatment modalities, and prognosis. Ann Surg Oncol 2012;19(9):2869–76.
26. Jarnagin WR, et al. Combined hepatocellular and cholangiocarcinoma: demographic, clinical, and prognostic factors. Cancer 2002;94(7):2040–6.
27. Sammon J, et al. MRI features of combined hepatocellular- cholangiocarcinoma versus mass forming intrahepatic cholangiocarcinoma. Cancer Imaging 2018;18(1):8.
28. de Campos RO, et al. Combined hepatocellular carcinoma-cholangiocarcinoma: report of MR appearance in eleven patients. J Magn Reson Imaging 2012;36(5):1139–47.
29. Hwang J, et al. Differentiating combined hepatocellular and cholangiocarcinoma from mass-forming intrahepatic cholangiocarcinoma using gadoxetic acid-enhanced MRI. J Magn Reson Imaging 2012;36(4):881–9.
30. Fowler KJ, et al. Combined hepatocellular and cholangiocarcinoma (biphenotypic) tumors: imaging features and diagnostic accuracy of contrast-enhanced CT and MRI. AJR Am J Roentgenol 2013;201(2):332–9.
31. Potretzke TA, et al. imaging features of biphenotypic primary liver carcinoma (hepatocholangiocarcinoma) and the potential to mimic hepatocellular carcinoma: LI-RADS analysis of CT and MRI features in 61 cases. AJR Am J Roentgenol 2016;207(1):25–31.
32. Aoki K, et al. Combined hepatocellular carcinoma and cholangiocarcinoma: clinical features and

computed tomographic findings. Hepatology 1993; 18(5):1090–5.
33. Jeon TY, et al. The value of gadobenate dimeglumine-enhanced hepatobiliary-phase MR imaging for the differentiation of scirrhous hepatocellular carcinoma and cholangiocarcinoma with or without hepatocellular carcinoma. Abdom Imaging 2010;35(3):337–45.
34. Wells ML, et al. Biphenotypic hepatic tumors: imaging findings and review of literature. Abdom Imaging 2015;40(7):2293–305.
35. Maximin S, et al. Current update on combined hepatocellular-cholangiocarcinoma. Eur J Radiol Open 2014;1:40–8.
36. Ohtsuka M, et al. Similarities and differences between intraductal papillary tumors of the bile duct with and without macroscopically visible mucin secretion. Am J Surg Pathol 2011;35(4):512–21.
37. Kloek JJ, et al. A comparative study of intraductal papillary neoplasia of the biliary tract and pancreas. Hum Pathol 2011;42(6):824–32.
38. Egri C, et al. intraductal papillary neoplasm of the bile duct: multimodality imaging appearances and pathological correlation. Can Assoc Radiol J 2017;68(1):77–83.
39. Katabathina VS, et al. Biliary diseases with pancreatic counterparts": cross-sectional imaging findings. Radiographics 2016;36(2):374–92.
40. Kang MJ, et al. Impact of macroscopic morphology, multifocality, and mucin secretion on survival outcome of intraductal papillary neoplasm of the bile duct. J Gastrointest Surg 2013;17(5):931–8.
41. Fuente I, et al. intraductal papillary neoplasm of the bile duct (IPNB): case report and literature review of a challenging disease to diagnose. J Gastrointest Cancer 2019;50(3):578–82.
42. Luvira V, et al. Long-term outcome of surgical resection for intraductal papillary neoplasm of the bile duct. J Gastroenterol Hepatol 2017;32(2):527–33.
43. Ohtsuka M, et al. Intraductal papillary neoplasms of the bile duct. Int J Hepatol 2014;2014:459091.
44. Park HJ, et al. Intraductal papillary neoplasm of the bile duct: clinical, imaging, and pathologic features. AJR Am J Roentgenol 2018;211(1):67–75.
45. Wu CH, et al. Comparative radiological pathological study of biliary intraductal tubulopapillary neoplasm and biliary intraductal papillary mucinous neoplasm. Abdom Radiol (NY) 2017; 42(10):2460–9.
46. Lim JH, et al. Cyst-forming intraductal papillary neoplasm of the bile ducts: description of imaging and pathologic aspects. AJR Am J Roentgenol 2011;197(5):1111–20.
47. Ogawa H, et al. CT findings of intraductal papillary neoplasm of the bile duct: assessment with multiphase contrast-enhanced examination using multi-detector CT. Clin Radiol 2012;67(3):224–31.
48. Wan XS, et al. Intraductal papillary neoplasm of the bile duct. World J Gastroenterol 2013;19(46): 8595–604.
49. Hong GS, et al. Thread sign in biliary intraductal papillary mucinous neoplasm: a novel specific finding for MRI. Eur Radiol 2016;26(9):3112–20.
50. Lim JH, Jang KT, Choi D. Biliary intraductal papillary-mucinous neoplasm manifesting only as dilatation of the hepatic lobar or segmental bile ducts: imaging features in six patients. AJR Am J Roentgenol 2008;191(3):778–82.
51. Schlitter AM, et al. Intraductal papillary neoplasms of the bile duct: stepwise progression to carcinoma involves common molecular pathways. Mod Pathol 2014;27(1):73–86.
52. Bosman FT, World Health Organization., International Agency for Research on Cancer. WHO classification of tumours of the digestive system. In: World Health Organization classification of tumours. 4th edition. Lyon: International Agency for Research on Cancer; 2010. p. 417.
53. Boyum JH, et al. Hepatic mucinous cystic neoplasm versus simple biliary cyst: assessment of distinguishing imaging features using CT and MRI. AJR Am J Roentgenol 2021;216(2):403–11.
54. Choi HK, et al. Differential diagnosis for intrahepatic biliary cystadenoma and hepatic simple cyst: significance of cystic fluid analysis and radiologic findings. J Clin Gastroenterol 2010;44(4): 289–93.
55. Arnaoutakis DJ, et al. Management of biliary cystic tumors: a multi-institutional analysis of a rare liver tumor. Ann Surg 2015;261(2):361–7.
56. Simo KA, et al. Invasive biliary mucinous cystic neoplasm: a review. HPB (Oxford) 2012;14(11): 725–40.
57. Sang X, et al. Hepatobiliary cystadenomas and cystadenocarcinomas: a report of 33 cases. Liver Int 2011;31(9):1337–44.
58. Kim HJ, et al. CT differentiation of mucin-producing cystic neoplasms of the liver from solitary bile duct cysts. AJR Am J Roentgenol 2014;202(1):83–91.
59. Kovacs MD, et al. Differentiating biliary cystadenomas from benign hepatic cysts: Preliminary analysis of new predictive imaging features. Clin Imaging 2018;49:44–7.
60. Seo JK, et al. Appropriate diagnosis of biliary cystic tumors: comparison with atypical hepatic simple cysts. Eur J Gastroenterol Hepatol 2010; 22(8):989–96.
61. Hagiwara K, et al. Resected primary mucinous cholangiocarcinoma of the liver. Surg Case Rep 2018;4(1):41.
62. Sumiyoshi T, et al. Mucinous cholangiocarcinoma: clinicopathological features of the rarest type of cholangiocarcinoma. Ann Gastroenterol Surg 2017;1(2):114–21.

63. Hayashi M, et al. Imaging findings of mucinous type of cholangiocellular carcinoma. J Comput Assist Tomogr 1996;20(3):386–9.
64. King MJ, et al. Outcomes assessment in intrahepatic cholangiocarcinoma using qualitative and quantitative imaging features. Cancer Imaging 2020;20(1):43.
65. Scarsbrook AF, et al. Anatomic and functional imaging of metastatic carcinoid tumors. Radiographics 2007;27(2):455–77.
66. Touloumis Z, et al. Primary hepatic carcinoid; a diagnostic dilemma: a case report. Cases J 2008; 1(1):314.
67. Quartey B. Primary hepatic neuroendocrine tumor: what do we know now? World J Oncol 2011;2(5): 209–16.
68. Lin CW, et al. Primary hepatic carcinoid tumor: a case report and review of the literature. Cases J 2009;2(1):90.
69. Nikfarjam M, Muralidharan V, Christophi C. Primary hepatic carcinoid tumours. HPB (Oxford) 2004; 6(1):13–7.
70. Gravante G, et al. Primary carcinoids of the liver: a review of symptoms, diagnosis and treatments. Dig Surg 2008;25(5):364–8.
71. Kim JE, et al. Three-phase helical computed tomographic findings of hepatic neuroendocrine tumors: pathologic correlation with revised WHO classification. J Comput Assist Tomogr 2011; 35(6):697–702.
72. Yang K, et al. Primary hepatic neuroendocrine tumors: multi-modal imaging features with pathological correlations. Cancer Imaging 2017;17(1):20.
73. Orlefors H, et al. Whole-body (11)C-5-hydroxytryptophan positron emission tomography as a universal imaging technique for neuroendocrine tumors: comparison with somatostatin receptor scintigraphy and computed tomography. J Clin Endocrinol Metab 2005;90(6):3392–400.
74. Koyama T, et al. Primary hepatic angiosarcoma: findings at CT and MR imaging. Radiology 2002; 222(3):667–73.
75. Yang KF, et al. Primary hepatic angiosarcoma: difficulty in clinical, radiological, and pathological diagnosis. Med J Malaysia 2012;67(1):127–8.
76. Thampy R, et al. Imaging features of rare mesenychmal liver tumours: beyond haemangiomas. Br J Radiol 2017;90(1079):20170373.
77. Chung YE, et al. Varying appearances of cholangiocarcinoma: radiologic-pathologic correlation. Radiographics 2009;29(3):683–700.
78. Epelboym Y, et al. Imaging findings in epithelioid hemangioendothelioma. Clin Imaging 2019;58: 59–65.
79. Alomari AI. The lollipop sign: a new cross-sectional sign of hepatic epithelioid hemangioendothelioma. Eur J Radiol 2006;59(3):460–4.
80. Wu CH, et al. Uncommon liver tumors: case report and literature review. Medicine (Baltimore) 2016; 95(39):e4952.
81. Ito Y, et al. A case report of primary fibrosarcoma of the liver. Gastroenterol Jpn 1990;25(6):753–7.
82. Huang ML, et al. Hepatic fibrosarcoma in a middle-aged man. Int J Clin Exp Pathol 2019;12(9): 3555–9.
83. Ali S, et al. Primary fibrosarcoma of the liver: we don't know much: a case report. Case Rep Gastroenterol 2008;2(3):384–9.
84. Chi M, Dudek AZ, Wind KP. Primary hepatic leiomyosarcoma in adults: analysis of prognostic factors. Onkologie 2012;35(4):210–4.
85. Emile JF, et al. Primary non-Hodgkin's lymphomas of the liver with nodular and diffuse infiltration patterns have different prognoses. Ann Oncol 2001; 12(7):1005–10.
86. Ferrozzi F, et al. Primary liver leiomyosarcoma: CT appearance. Abdom Imaging 1996;21(2):157–60.
87. Yu RS, et al. Primary hepatic sarcomas: CT findings. Eur Radiol 2008;18(10):2196–205.
88. Restrepo CS, et al. Imaging manifestations of Kaposi sarcoma. Radiographics 2006;26(4): 1169–85.
89. Luburich P, et al. Hepatic Kaposi sarcoma in AIDS: US and CT findings. Radiology 1990;175(1):172–4.
90. Kim KA, et al. Unusual mesenchymal liver tumors in adults: radiologic-pathologic correlation. AJR Am J Roentgenol 2006;187(5):W481–9.
91. Caccamo D, Pervez NK, Marchevsky A. Primary lymphoma of the liver in the acquired immunodeficiency syndrome. Arch Pathol Lab Med 1986; 110(6):553–5.
92. Padhan RK, Das P, Shalimar. Primary hepatic lymphoma. Trop Gastroenterol 2015;36(1):14–20.
93. Apter S, et al. Calcification in lymphoma occurring before therapy: CT features and clinical correlation. AJR Am J Roentgenol 2002;178(4):935–8.
94. Ippolito D, et al. Diagnostic approach in hepatic lymphoma: radiological imaging findings and literature review. J Cancer Res Clin Oncol 2020; 146(6):1545–58.
95. Colagrande S, et al. MRI features of primary hepatic lymphoma. Abdom Radiol (NY) 2018;43(9):2277–87.
96. Kharuzhyk S, et al. Comparison of whole-body MRI with diffusion-weighted imaging and PET/CT in lymphoma staging. Eur Radiol 2020;30(7):3915–23.
97. Abbas F, et al. Post-transplantation lymphoproliferative disorders: current concepts and future therapeutic approaches. World J Transpl 2020;10(2): 29–46.
98. Pickhardt PJ, Siegel MJ. Posttransplantation lymphoproliferative disorder of the abdomen: CT evaluation in 51 patients. Radiology 1999;213(1):73–8.
99. Borhani AA, et al. Imaging of posttransplantation lymphoproliferative disorder after solid organ

transplantation. Radiographics 2009;29(4): 981–1000. discussion 1000-2.
100. Tomasian A, et al. Hematologic malignancies of the liver: spectrum of disease. Radiographics 2015; 35(1):71–86.
101. Singh A, et al. Role of diffusion weighted imaging in diagnosis of post transplant lymphoproliferative disorders: Case reports and review of literature. Indian J Nephrol 2016;26(3):212–5.
102. Horn SR, et al. Epidemiology of liver metastases. Cancer Epidemiol 2020;67:101760.
103. Del Poggio P, Buonocore M. Cystic tumors of the liver: a practical approach. World J Gastroenterol 2008;14(23):3616–20.
104. Borhani AA, Wiant A, Heller MT. Cystic hepatic lesions: a review and an algorithmic approach. AJR Am J Roentgenol 2014;203(6):1192–204.
105. Casillas VJ, et al. Imaging of nontraumatic hemorrhagic hepatic lesions. Radiographics 2000;20(2):367–78.
106. Siskind BN, et al. CT features of hemorrhagic malignant liver tumors. J Comput Assist Tomogr 1987;11(5):766–70.